Supplemental Information

for

# Unique Properties of DNA Duplexes Containing Interstrand Crosslinks

Joshua I. Friedman, Yu-Lin Jiang, Paul S. Miller, and James T. Stivers

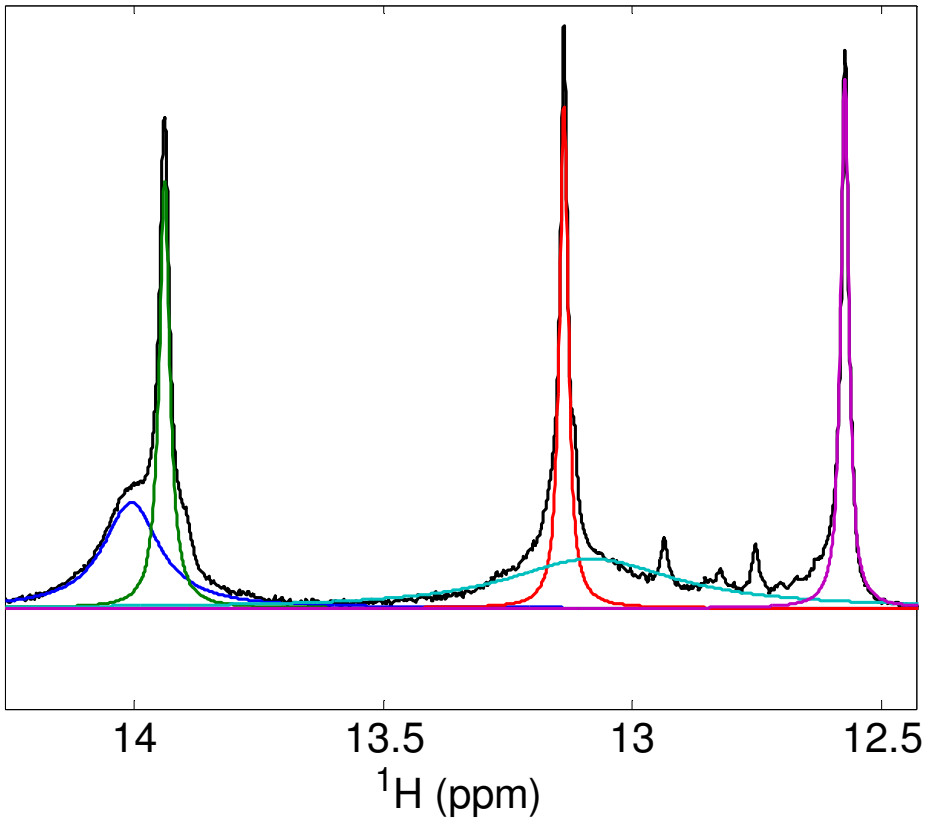


**Figure S1.** Nonlinear least squares minimied fit of the five imino protons of the CGX-12 dna to five lorentizan functions lorentizian lineshapes. The jump-return spectra were fitted to the summation of five lorenztian functions of the form: $\sum_{i=1}^{5} \frac{A_i}{\pi} \frac{\Gamma_i}{(x-x_i)^2+(\Gamma_i)^2}$ where $A_i$ is the amplitude, $x_i$ is the peak center position, and $\Gamma_i$ the linewidth of peak $i$. Analysis begins by measuring the linewidths of each peak in a fully relaxed spectrum employing a single amplitude factor that reflects the equal stoichmetries of each imino proton. When fitting imino exchange data, the amplitude factor for each imino proton was a floated variable. The best fit modeling of CGX-12 spectra is shown: T2 (blue), T8 (green), G6 (red), G12 (cyan), and G4 (purple).

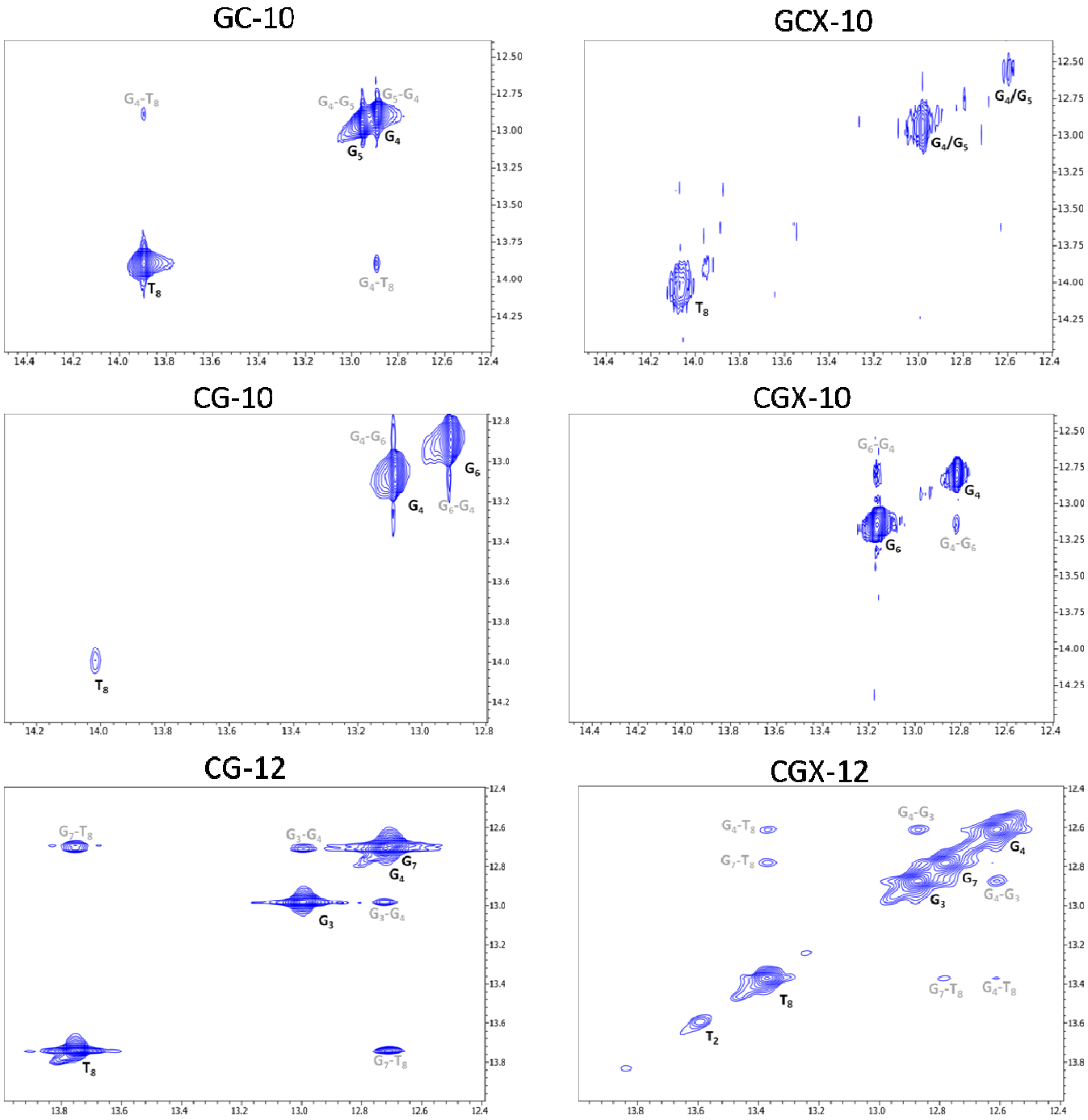


**Figure S2.** $^{1}$H-$^{1}$H NOESY spectra of the indicated DNA constructs (Fig. 3). Inter-imino NOE's are labeled in grey and peak assignments are in black.

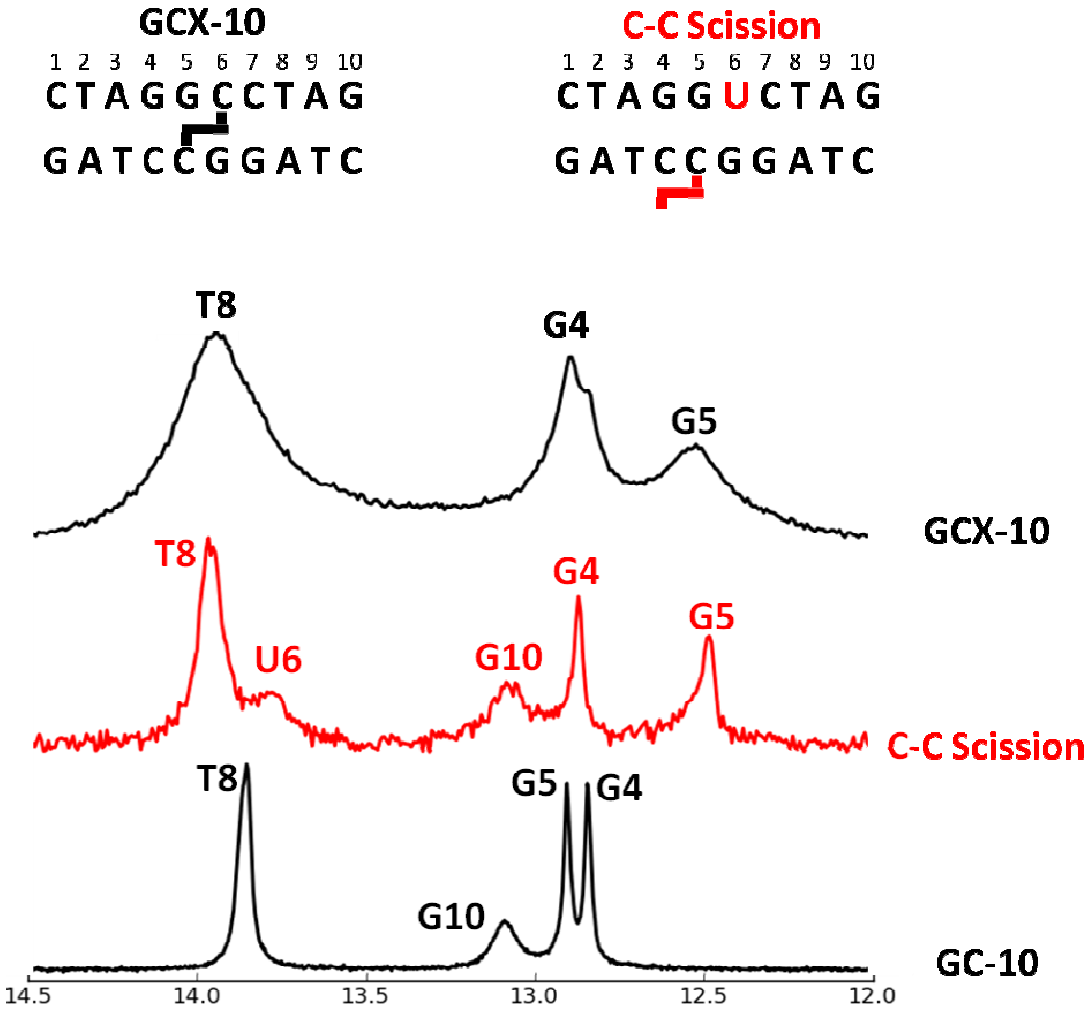


**Figure S3**. Comparison of the imino spectral regions of the GC-10, GCX-10, and the GCX-10 C-C scission product eight days following the imino proton exchange experiments (see text, red). The spectrum of the C-C scission product is consistent with N4 deamination of residue C6 on a single strand of each duplex. This scission breaks the symmetry of the duplex and converts C6 into a uracil base (U6), which appears greatly broadened in the spectrum due to its wobble base pairing with the opposite guanine. Reasonable assignments for the GCX-10 spectrum may be derived from the normal GC-10 and C-C-scission spectra: T8, G4 and G10 have similar shifts in all spectra (G10 is obscured in the GCX-10 spectrum); the distinct shift of G5 in the C-C scission and GCX-10 duplexes likely arises from its pairing with the alkylated N4 of the opposite C6 in these constructs. Although these are reasonable assignments, none of the conclusions are dependent on specific assignments in the GCX-10 duplex.

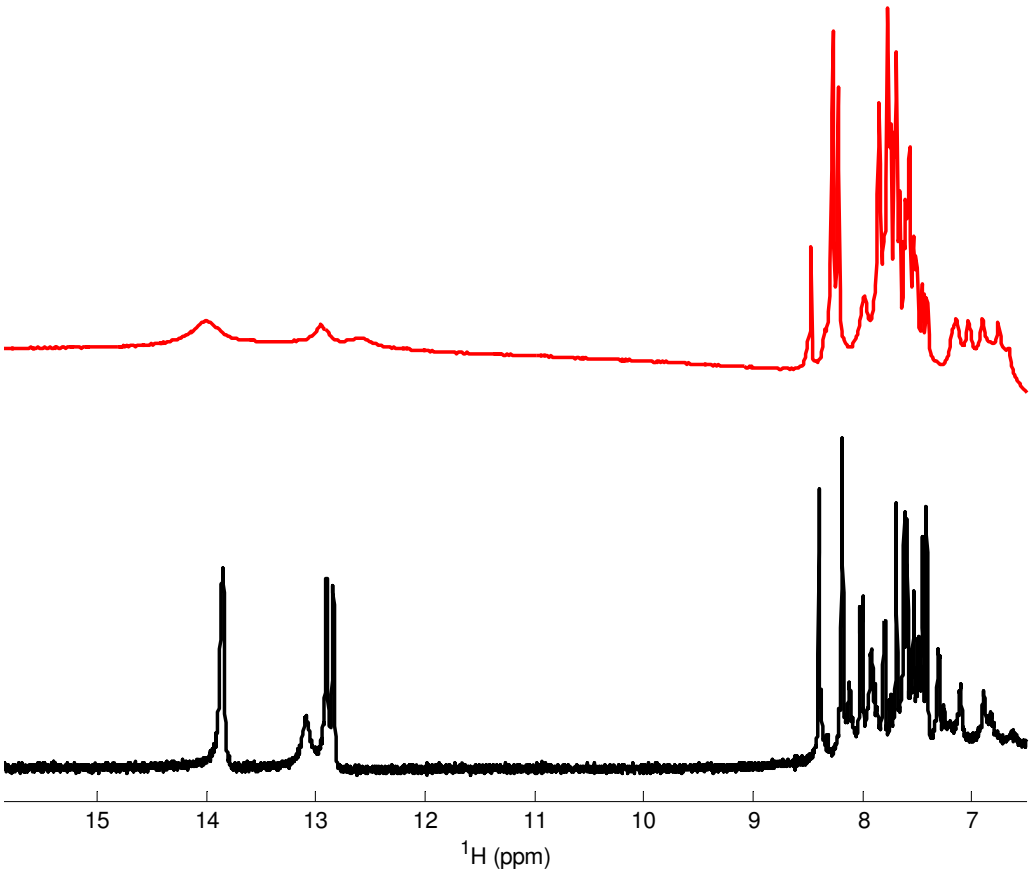


**Figure S4.** Downfield proton spectral regions of GCX-10 (red) and GC-10 (black). Spectra are normalized relative to the peak of greatest intensity in each spectrum. Although line broadening is apparent for non-exchangeable protons in GCX-10, this line broadening is small compared to the line broadening of its imino protons arising from their exchange with solvent.

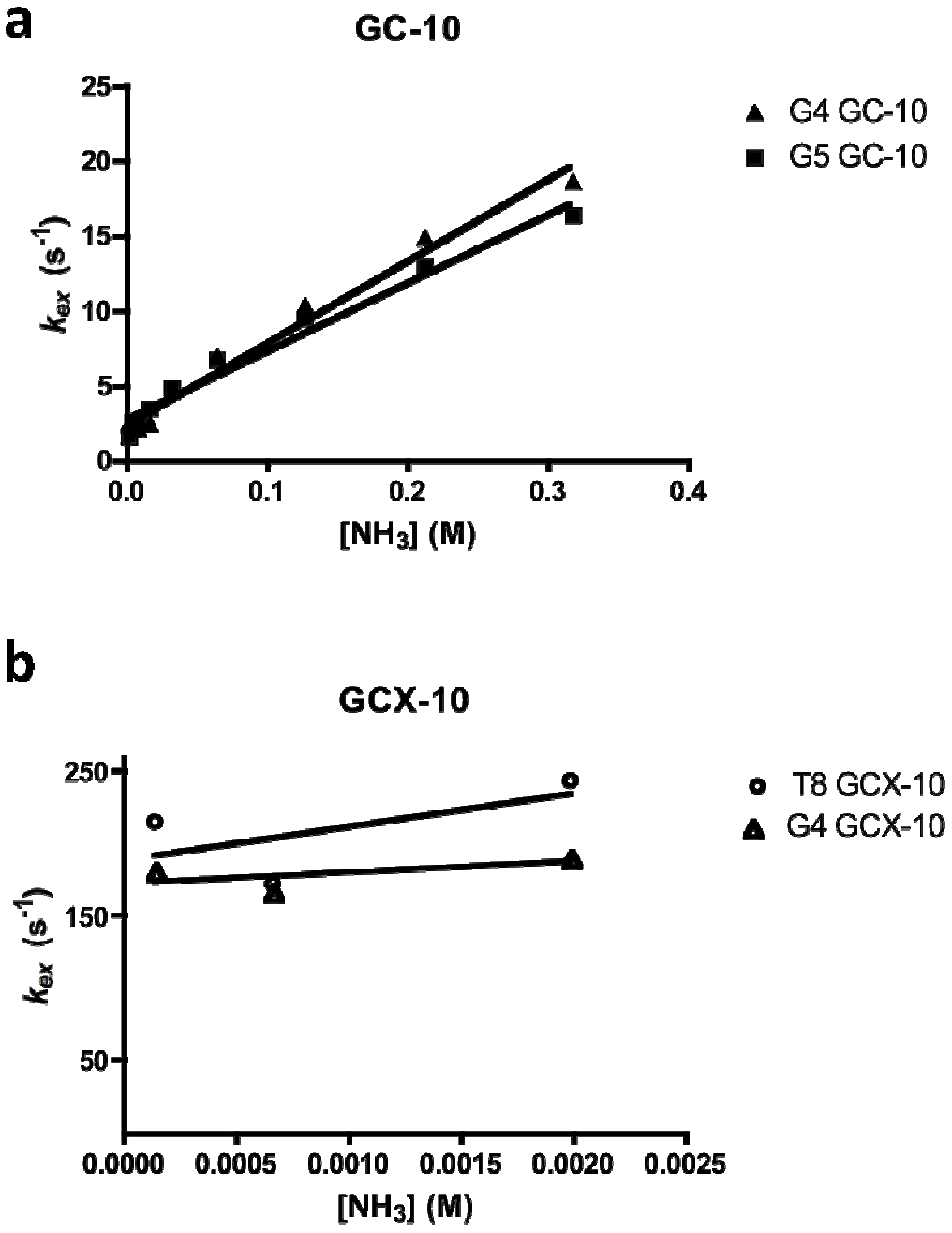


**Figure S5.** Rate of imino proto exchange as function of ammonia catalyst. (a) catalyst dependence of GC-10 immino proton exchange. (b) Catalyst dependence of GCX-10 immino proton exchange. Note the differences in scale between panel a and b. Black lines are the linear best fits of the data (eq 2, for concentrations of ammonia where $k_b \times [NH_3] << k_{cl}$ ).

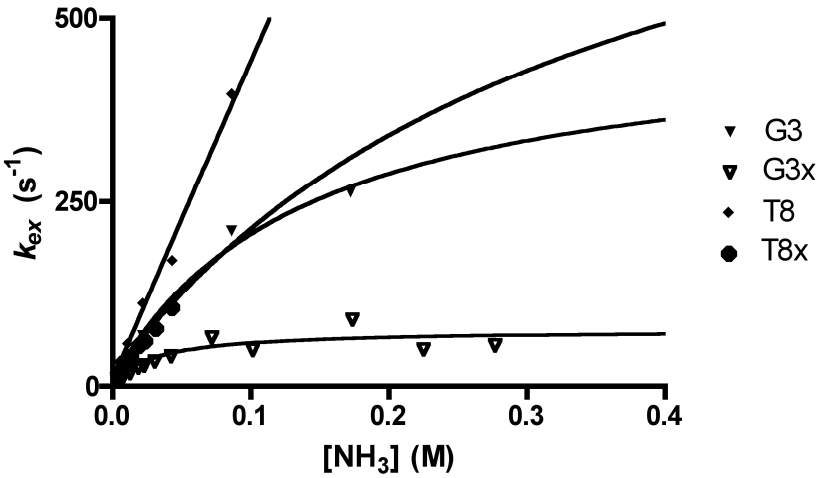


**Figure S6.** Apparent imino proton exchange rates as a function of [$NH_3$] catalyst for the fastest opening base pairs in the CG-12 and CGX-12 duplexes. Exchange rates less than 100 $s^{-1}$ were measured via magnetization transfer, and those greater than 100 $s^{-1}$ were derived from linewidth measurements. Curves are nonlinear least squares fits to eq2.